To be published in the Bulletin of the Seismological Society of America
Bull. Seismol. Soc. Am., 102(1), 343-351, 2012

Andaman Postseismic Deformation Observations: Still Slipping After All These Years?

J. Paul[1], C.P. Rajendran[2], A.R. Lowry[3], V. Andrade[2] and K. Rajendran[2]
[1]*University of Memphis, Memphis, Tennessee, 38654 USA*
[2]*Centre for Earth Sciences, Indian Institute of Science, Bangalore 560012, India*
[3]*Utah State University, Utah, 84322 USA*

Abstract: More than six years after the great (M_w 9.2) Sumatra-Andaman earthquake, post-event processes responsible for relaxation of the coseismic stress change remain controversial. Modeling of Andaman Islands Global Positioning System (GPS) displacements indicated early near-field motions were dominated by slip down-dip of the rupture, but various researchers ascribe elements of relaxation to dominantly poroelastic, dominantly viscoelastic and dominantly fault slip processes, depending primarily on their measurement sampling and modeling tools used. After subtracting a pre-2004 interseismic velocity, significant transient motion during the 2008.5-2010.5 epoch confirms that postseismic relaxation processes continue in Andaman. Modeling three-component velocities as viscoelastic flow yields a weighted root-mean-square (WRMS) misfit that always exceeds the WRMS 26.3 mm/yr of the measured signal. The best-fitting models are those that yield negligible deformation, indicating the model parameters have no real physical meaning. GPS velocities are well-fit (WRMS 4.0 mm/yr) by combining a viscoelastic flow model that best-fits the horizontal velocities with ~50 cm/yr thrust slip downdip of the coseismic rupture. Both deep slip and flow respond to stress changes, and each can significantly change stress in the realm of the other, so it is reasonable to expect that both transient deep slip and viscoelastic flow will influence surface deformation long after a great earthquake.

Introduction

The December 26th 2004, M_w 9.2 Sumatra-Andaman earthquake ruptured more than 1300 km of the subduction megathrust along the eastern boundary of the Indian and Australian plates (e.g., Shearer and Bürgmann, 2010). Coseismic and postseismic Global Positioning System (GPS) observations within the large rupture area provide an unusual opportunity to examine the nature of postseismic deformation. The nearly 500 km-long Andaman segment (Figure 1), the northernmost stretch of the 2004 event, evidenced slower rupture propagation (Banerjee *et al.*, 2005, Lay *et al.*, 2005) and less slip (Chlieh *et al.*, 2007) than other segments. The Andaman Islands span a lateral distance from ~20 km up-dip to ~30 km downdip of the base of coseismic rupture (Paul *et al.*, 2007). This coupled with availability of pre-earthquake GPS velocities makes the Andaman segment an ideal location for continuous observation of near-field postseismic relaxation processes (Paul *et al.*, 2007; Rajendran *et al.*, 2007).

Transient postseismic motions result from stress relaxation processes that include: (1) aseismic slip in zones of stable friction within or down-dip of the coseismic rupture (Tse and Rice, 1986); (2) viscoelastic flow in the ductile regime (Rundle, 1978) and (3) poroelastic redistribution of pore-fluid pressure (Peltzer *et al.*, 1998; Jonsson *et al.*, 2003). Postseismic signals following great earthquakes likely reflect all three processes, but no prior measurements of postseismic deformation following M_w > 9 earthquakes sample densely in both time and space. Thus, the 2004 Sumatra-Andaman event ultimately will provide an important data point for understanding the relative roles of these three processes in the earthquake cycle.

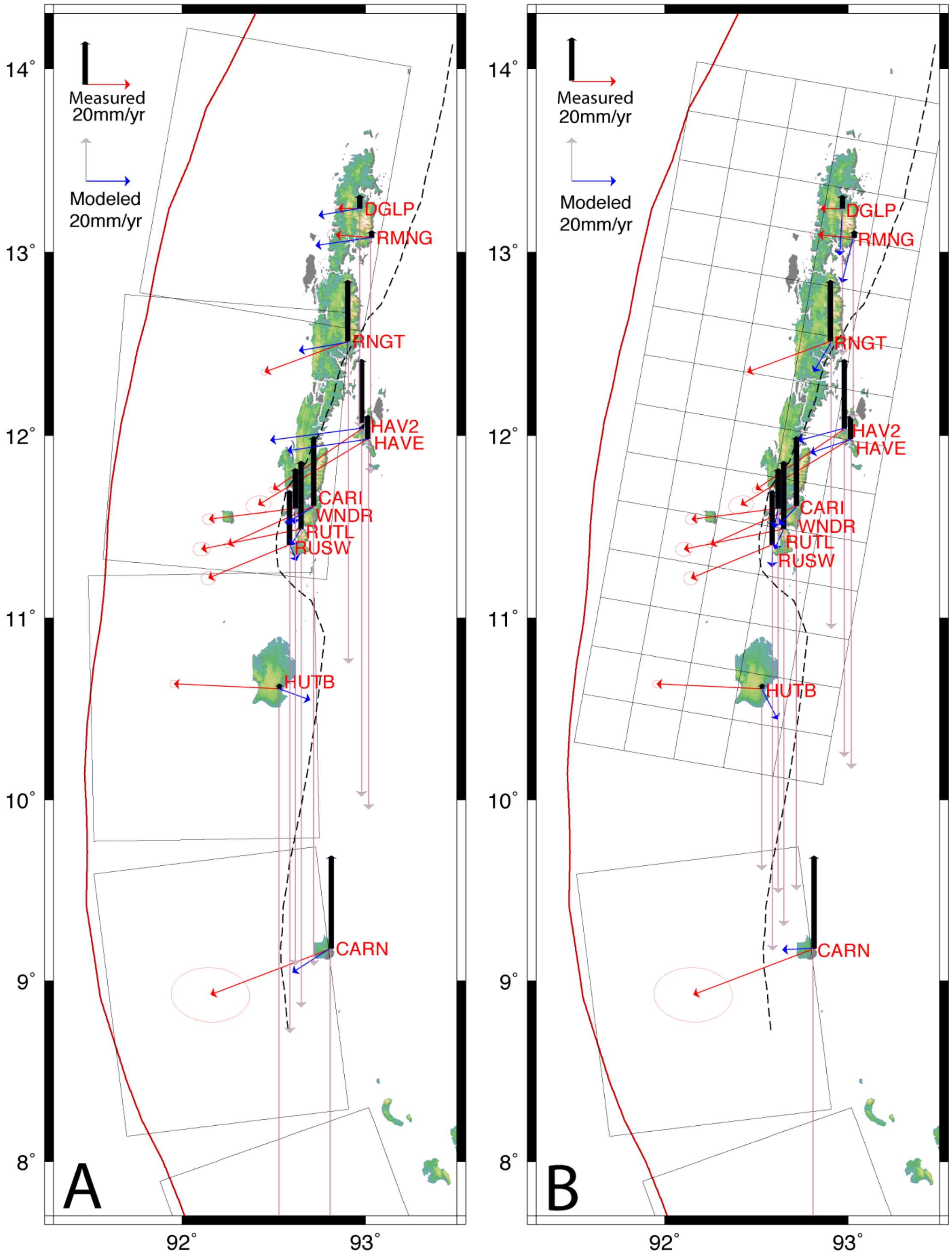

Figure 1: *Location map. The eleven Andaman network GPS sites with measured transient velocities for the 2008.5-2010.5 epoch (red vectors are horizontal; black bars are vertical). The hinge line separating coseismic subsidence from uplift (Meltzner et al., 2006) is dashed. A. Blue vectors (horizontal) and grey bars (vertical) show 2008.5-2010.5 epoch velocities predicted for a viscoelastic response model that best-fit the horizontal velocities, assuming a coarsely-discretized, eight segment coseismic rupture (dislocation planes outlined in grey). B. Similar to (A) but using a finer discretization of the coseismic rupture in the Andaman near-field.*

A majority of research groups interpreted rapid slip as the dominant transient process in GPS measurements during the first several months after the earthquake. Short-term postseismic slip was inferred based on near-field (Andaman and Nicobar islands) GPS measurements (Gahalaut *et al*., 2006; Banerjee *et al*., 2007; Gahalaut, Catherine, *et al*., 2008), near-field uplift observed from biological markers and eyewitness accounts (Kayanne *et al.*, 2007), and far-field GPS time series (Vigny *et al.*, 2005; Hashimoto *et al*., 2006; Kreemer *et al*., 2006; Chlieh *et al*., 2007). Paul *et al*. (2007) concluded slip processes dominated Andaman near-field GPS measurements on longer timescales of more than a year: They modeled all three relaxation processes but found only postseismic slip replicated near-field uplift and strain observed in Andaman GPS data during the first two years post-event. Postseismic slip in their model (and others, e.g., Gahalaut, Jade, *et al.*, 2008; Chlieh *et al*., 2007) overlapped slightly with coseismic, but most of the moment release occurred further downdip, consistent with expectations based on frictional models of the earthquake cycle (e.g., Tse and Rice, 1986; Lapusta *et al*., 2000; Liu and Rice, 2007).

Several studies examined a viscoelastic mechanism for postseismic deformation following the 2004 event. Pollitz *et al*. (2006) modeled the first four months of GPS motion at far-field sites with a biviscous rheology, but that model predicted subsidence at near-field Andaman and Nicobar Island sites, opposite the observed GPS vertical (Figure 2). Pollitz *et al*. (2008) expanded the viscoelastic model to include three-dimensional structure (a high-viscosity slab and relatively low-viscosity supra-slab asthenospheric wedge), which they compared to both near-field and far-field GPS observations. The laterally-varying viscosity structure improved overall fits to GPS time series and produced slight (1-2 cm over the first year) near-field uplift instead of subsidence, but did not reproduce the large (10-25 cm) observed uplift in the Andaman-Nicobar islands.

Other analyses examined the postseismic transient observed in Gravity Recovery and Climate Experiment (GRACE) time-variable geoid data (Ogawa and Heki, 2007; Chen *et al*., 2007; Han *et al*., 2008; Cannelli *et al*., 2008; de Linage *et al*., 2009; Panet *et al*., 2010; Einarsson *et al*., 2010). Of the gravity studies that expressed a strong preference for a relaxation mechanism, most chose biviscous viscoelastic flow (e.g., Han *et al*., 2008; Panet *et al*., 2010; Einarsson *et al*., 2010), but these studies also noted that small amounts of slip would be necessary to promote the near-field GPS observations of uplift. The principal exception was Ogawa and Heki (2007), who interpreted the transient they estimated from GRACE geoid time series as representing a mix of afterslip and poroelastic water mass flux in the mantle.

In some respects, results of postseismic analyses thus far resemble the ancient tale of the blind men and the elephant: The perception of truth is flavored by where (and when) the measurements are made. However the overall consensus holds that short-term (< ~1 year) and/or near-field GPS measurements are dominated by postseismic slip, whereas longer-term GRACE and GPS time series reflect a dominantly viscoelastic response. In this paper we present observations from eleven of the fifteen GPS stations we operate in the Andaman Islands, and we examine the likely nature of current deformation in the region.

GPS Measurements

Fifteen GPS sites are currently maintained by our group in the Andaman Islands, five sampling continuously and eight intermittently, to measure postseismic deformation following the 2004 earthquake. Concrete pillar monuments for the continuous sites are constructed from designs suggested by the University Navstar Consortium (UNAVCO). Campaign sites consist of a 6-inch stainless steel pin driven into the hardest rock possible in Andaman and anchored with epoxy. Each campaign measurement consists of three to five 24-hour daily observations to minimize multipath effects, which are problematic at many Andaman sites where trees and hilly slopes surround the sites. GPS data were analyzed using GAMIT/GLOBK software with Massachusetts Institute of Technology (MIT) final orbits and forty fiducial sites in the 2005 International Terrestrial Reference Frame (ITRF2005; Altamimi *et al*., 2007), and combined using MIT h-files (Herring, 2003). Thirteen reference frame sites of the ITRF2005 were used to stabilize the network. ITRF2005 GPS velocities for the 2008.5-2010.5 epoch were estimated at eleven sites in Andaman and Nicobar using GLOBK. The ITRF2005 interseismic velocity of a site in Port Blair (for a 1996-2000 pre-earthquake epoch) was subtracted from post-2004 time-series to isolate the postseismic transient suitable for modeling. Examples of these time series at four sites are shown in Figure 2. All time series and velocities depicted, discussed and modeled in this paper are motions referenced to the interseismic in this manner.

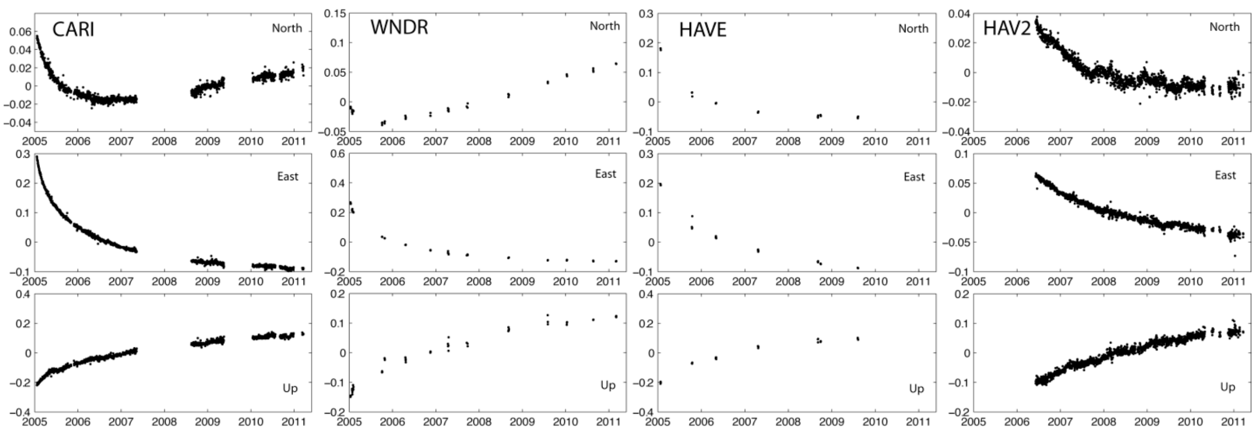

Figure 2: *Example GPS time series of postseismic transient deformation, for sites CARI (left panels), WNDR (center-left), HAVE (center-right) and HAV2 (right) in central Andaman Islands. North is top, east if middle and vertical is at the bottom in the figure. All sites in Andaman continue to rise after six years.*

Continuous GPS recording, initiated two to six weeks after the earthquake, documents persistent uplift and SW to WSW transient motion. For example, CARI rose by ~23 cm in first two years (Paul *et al*., 2007). This trend continues to the present, although at a much lower rate than in earlier years. As of the middle of 2010, sites near Port Blair had risen more than 35 cm, a >40% reversal of coseismic subsidence (Figure 2). Sites initially moved in approximately the same horizontal direction as their coseismic displacement, but over the last several years they have gradually adopted a more northerly velocity. Despite the limited land exposure on the islands, the postseismic displacements exhibit significant spatial variations.

Modeling

For this analysis, we use VISCO1D (Pollitz, 1997) to model contributions to GPS site motions from viscoelastic relaxation during the most recent (2008.5–2010.5) two-year epoch of measurements. VISCO1D models viscoelastic flow in a radially-symmetric, self-gravitating spherical Earth. The surface response to viscoelastic flow depends on Earth material properties and on forcing by the coseismic stress change. To estimate unknown material properties, we examined models with elastic layer thicknesses ranging from 40 to 100 km, and upper mantle

(<670 km depth) Maxwell viscosities, η_{UM}, ranging from 10^{16} to 10^{21} Pa s. We assumed a lower mantle viscosity of 10^{21} Pa s.

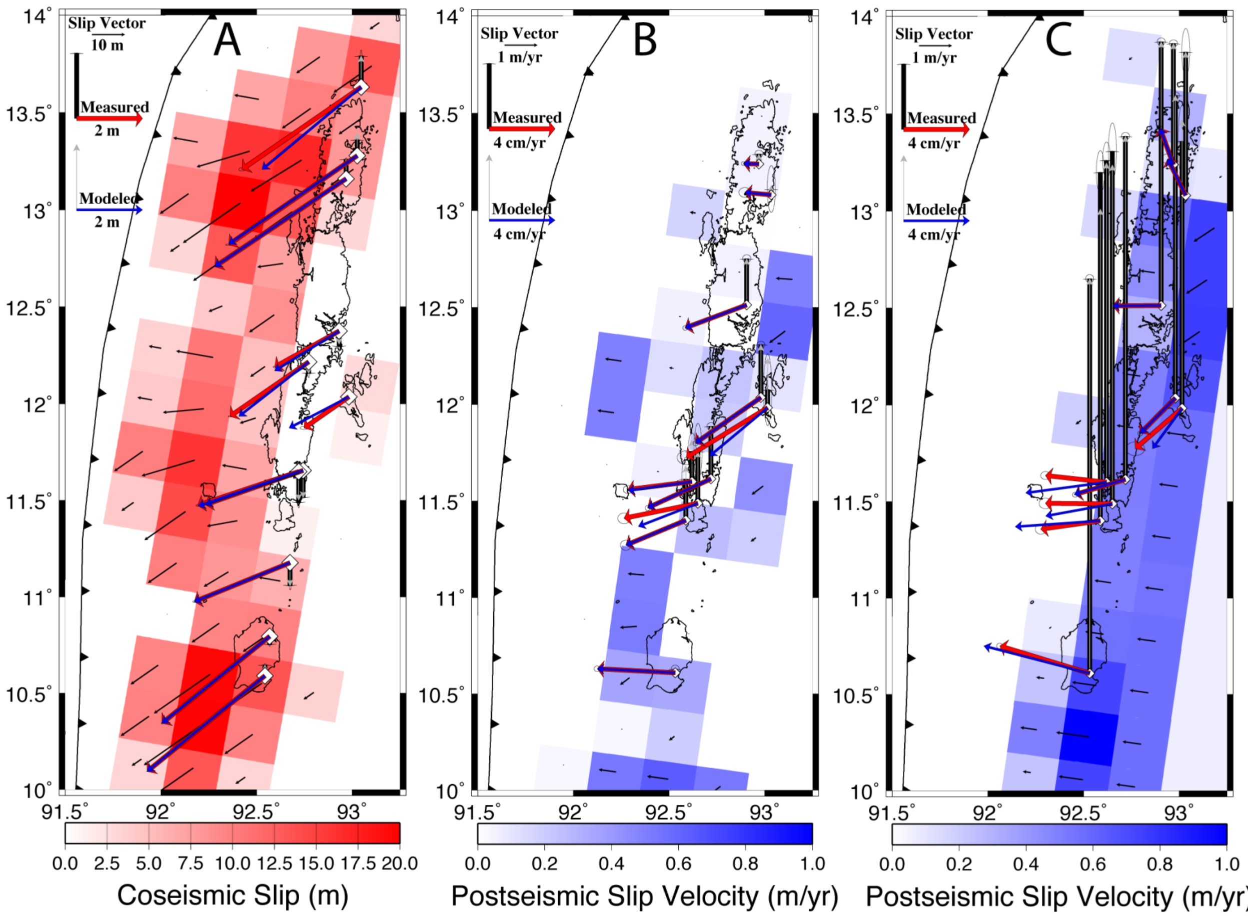

Figure 3: *Slip models of Andaman GPS measurements. A. Coseismic slip model of Paul et al. (2007), used in the "fine model" of viscoelastic forcing. B. Best-fitting slip model of the 2008.5-2010.5 epoch measured transient GPS velocities. C. Best-fitting slip model of residual velocities after subtracting the viscoelastic model that best-fit the measured horizontal velocities (η_{UM} = 3×10^{17} Pa s; elastic layer thickness = 90 km. The viscoelastic model velocity predictions are shown in Figure 1b).*

The coseismic stress change depends on the slip distribution, which can be constrained independently from modeling of coseismic deformation, tsunami propagation and/or seismic waveforms. To examine the sensitivity of model results to uncertainties in the slip distribution, we examine postseismic deformation excited by two different coseismic slip models. Both models use four large slip dislocations derived from combined modeling of seismic waveforms and tsunami (supplementary materials in Lay *et al*., 2005) to describe the southern part of the rupture (south of 8°N latitude). At those large distances, our postseismic measurements are sensitive only to the centroid moment tensor and not to finer-scale details of the slip distribution. In the first coseismic slip model (Figure 1a, hereafter referred to as the "coarse model"), the northern half of the rupture is represented by four large (160×140 km) slip dislocations derived from far-field coseismic GPS measurements (Banerjee *et al*., 2007). The second model of coseismic slip (Figure 1b, the "fine model") replaces the northernmost three dislocations in the coarse model with a constrained inversion of the near-field Andaman and Nicobar GPS data for slip on seventy 30×30 km patches near Andaman Islands, as described in Paul *et al*. (2007); the slip distribution is reproduced in Figure 3a. Differences in the predictions from these two models can be considered representative of the uncertainties in near-field viscoelastic deformation introduced by uncertainties in the coseismic slip distribution.

Figure 4 depicts the weighted root-mean-square (WRMS) misfit error for the analyses. Figures 4a and 4b depict the full misfit (including all three components of velocity) for the coarse model and the fine model respectively, while Figures 4c and 4d show the WRMS misfit when the vertical velocity is neglected. Significantly, no model reproduces the large rates of uplift that we continue to observe at almost all GPS sites, as illustrated by the differences between the upper and lower panels of Figure 4. The coarse and fine coseismic slip models produce very similar misfit surfaces, demonstrating that uncertainties in the coseismic slip distribution inverted from coseismic GPS measurements contribute relatively little to the overall misfit in viscoelastic models.

When all three components of velocities are used, the WRMS misfits are greater than or equal to the 26.3 mm/yr WRMS of the measured signal for all parameter combinations, and for both of the coseismic slip models. There is no single error minimum for either Figure 4a or 4b: Essentially, every viscoelastic model that predicts negligible deformation during the 2008.5-2010.5 epoch of observations yields the "global minimum misfit" equaling the WRMS of the observations. This pattern of behavior appears to result from the radially-symmetric model prediction of significant subsidence near the downdip terminus of rupture where we observe uplift.

The best-fit parameters for the comparisons in Figure 4c and 4d using only the horizontal velocities, 3×10^{17}–10^{18} Pa s upper mantle viscosity beneath a 90 km elastic layer, are consistent with estimates derived from gravity and far-field GPS estimates (viscosities in the range 5×10^{17}–10^{19} Pa s, with lower values being the transient end-member of biviscous models, and elastic layer thicknesses ~ 40–60 km). A thicker elastic layer here is not surprising, as the near-field source-measurement sampling should more uniquely reflect the local rheology (e.g., Paulson *et al*., 2005) consisting of ~40 km of cold upper-plate over a thick and cold ~100 Myr-old oceanic slab, whereas the far-field measurements average over a variety of lithospheric profiles that include Andaman Sea back-arc rifting. Figure 1 compares the best-fitting viscoelastic rebound models from the horizontal velocity comparison to the observed transient postseismic GPS velocities. Even these models have rather large misfits however, with WRMS 20.9 and 23.7 mm/yr for the models depicted in Figure 1a and 1b respectively. These represent only a slight reduction of variance relative to the 26.6 mm/yr WRMS of the horizontal velocity measurements.

Discussion

The observed uplift in the Andaman region is opposite the uniformly downward prediction of the viscoelastic models, and these models also fit the horizontal motions very poorly. This suggests that other processes in addition to viscoelastic rebound play a significant role in defining the postseismic velocity field nearly six years after the earthquake. The obvious candidates are poroelastic relaxation, postseismic slip, and interseismic slip.

Ogawa and Heki's (2006) interpretation that GRACE geoid changes reflect poroelastic water mass redistribution in the mantle is at odds with relationships of Andaman vertical to horizontal GPS displacements, which are opposite those predicted for poroelastic deformation (Paul *et al*.,

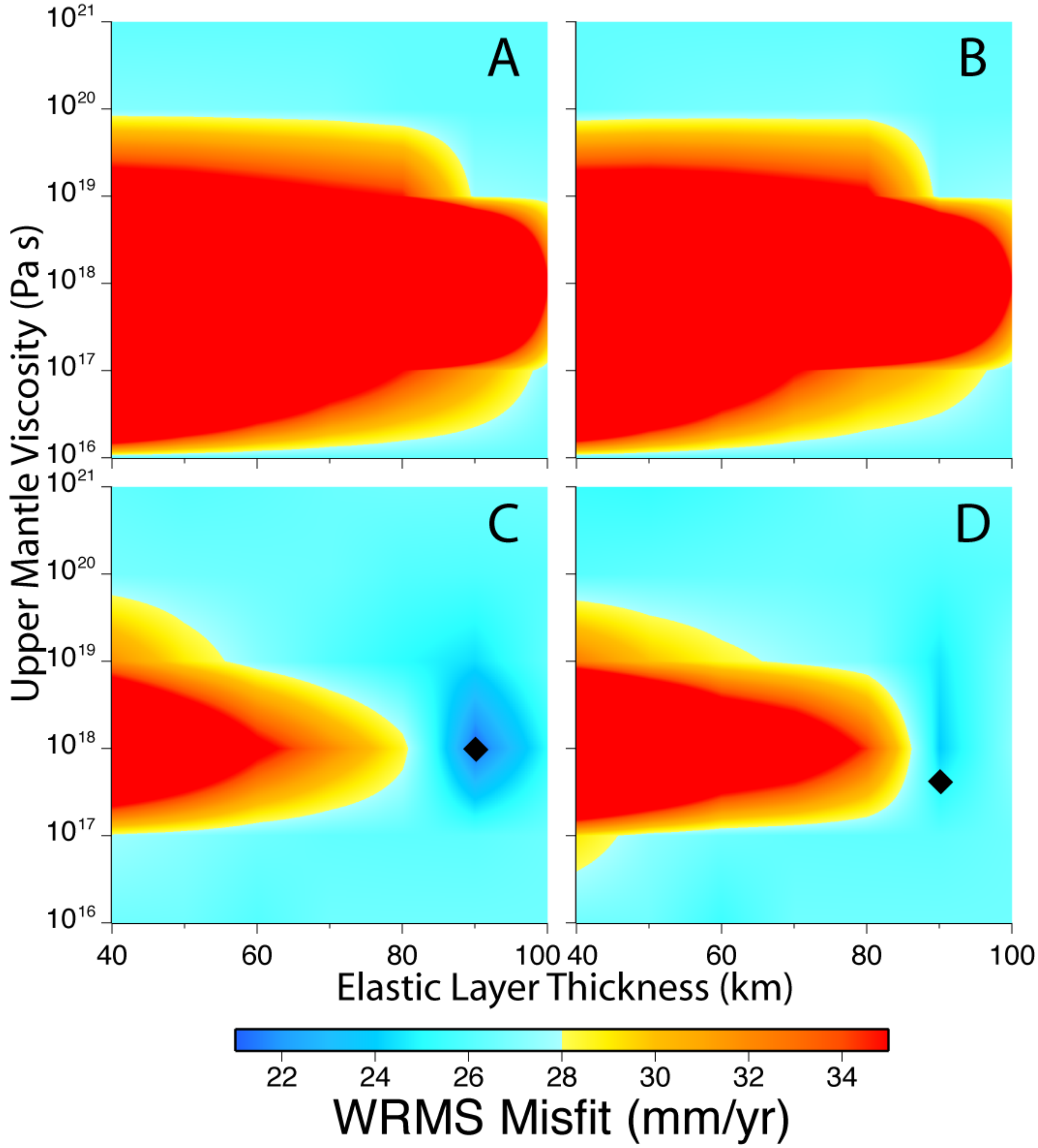

Figure 4. *Weighted root-mean-square misfit of viscoelastic relaxation models to observed velocities for the 2008.5-2010.5 epochs, as a function of model parameters (thickness of the elastic layer and upper mantle viscosity). Diamonds are minima. A. Misfit using three-component velocities and the "coarse model" of coseismic slip shown in Figure 1a. B. Misfit using three-component velocities and the "fine model" of coseismic slip shown in Figure 1b. C. Misfit using only horizontal velocities and the "coarse model". D. Misfit using only horizontal velocities and the "fine model". Differences between the top and bottom panels illustrate how the misfit is biased by the inability of radially symmetric viscoelastic models to reproduce observed vertical uplift.*

2007). Moreover, notwithstanding their argument for ~1% free water in the back-arc wedge, their model would require the water to be present in subducting oceanic mantle lithosphere. Hughes *et al*. (2009) modeled poroelastic effects expected for the Sumatra-Andaman event using reasonable estimates of porosities and permeabilities and found that pore-pressure effects dissipated over timescales of less than a month in fore-arc and back-arc regions, and of order several months in oceanic crust of the down-going slab. Consequently, it is reasonable to assume that poroelastic effects do not contribute significantly to anomalous motions during the past several years.

That leaves some combination of viscoelastic rebound and slip. Viscoelastic relaxation alone cannot explain the observed patterns of behavior, primarily because radial viscoelastic models predict subsidence where we observe very significant rates of transient uplift. The sites are atop or slightly downdip of the deep frictional transition on the megathrust, as evidenced by their proximity to the hinge line separating coseismic uplift from subsidence (Meltzner *et al*., 2006; see Figure 1). The hinge line should approximately correspond to the downdip limit of coseismic rupture and corresponds well to estimates of that limit derived from geodetic data (Paul *et al*., 2007; see also Figures 1a and 4a). The sense of shear strain is consistent with that expected for interseismic strain near the transition from frictionally coupled to sliding on the megathrust, given the obliquity of motion of India relative to the Andaman sliver. The oblique component of motion across the Andaman network changes by 20 mm/yr going from east to west across the network in the 2008.5-2010.5 epoch. Although we have no interseismic measurements of shear strain rates prior to 2004 (CARI was the sole location measured more than once prior to the great earthquake), 20 mm/yr is below the limit of 30-40 mm/yr for oblique plate motion of India relative Sundaland (Socquet *et al*., 2006). Some of that 30-40 mm/yr oblique motion between Andaman and Sunda is accommodated on the Sagaing fault and the Andaman Sea spreading center, both of which lie well west of our network. Nevertheless, one might reasonably ascribe the right-lateral shear strain across Andaman to “normal” interseismic behavior near the downdip transition from stick-slip to stable frictional sliding.

The vertical uplift cannot be easily dismissed as interseismic motion however. The measured velocities and displacements depicted in Figures 1 and 2 are shown relative to the pre-event velocity near CARI, so the 32 mm/yr uplift at CARI in the 2008.5–2010.5 epoch cannot be attributed to interseismic slip. As previously noted, radially symmetric models of viscoelastic response predict subsidence in the near-field. Pollitz *et al*. (2008) were able to produce small amounts of uplift (~10 mm in the first year) using a three-dimensional model with lower viscosity in the subduction zone’s asthenospheric wedge, but were still an order of magnitude less than the observed uplift during that period. They noted that the uplift could be increased by decreasing viscosity of the asthenospheric wedge or shifting the base of their coseismic rupture planes to the east, but these parameter changes would increase the misfit in other components or at other sites. Alternatively, the first two years of GPS motion at all Andaman sites were remarkably well-fit (WRMS misfit of 7 mm for all daily coordinates) by a model invoking only rapid, exponentially-decaying slip down-dip of the rupture zone (Paul *et al.*, 2007). The 2008.5–2010.5 velocities have a very similar expression (although the rates are roughly an order of magnitude less), so they should be readily fit by continued postseismic slip at roughly an order-of magnitude lower rate.

To test this possibility, we model in Figure 3 the 2008.5–2010.5 velocities using the same minimum moment inversion methodology described previously in Paul *et al*. (2007). For comparison, the coseismic slip distribution inverted by Paul *et al*. (2007) is reproduced in Figure

3a. We consider two end-member models for the postseismic slip: In the first model (Figure 3b), all of the observed 2008.5-2010.5 deformation is inverted (i.e., we assume that there is no viscoelastic flow contribution to the velocities). This yields as much as 60 cm/yr of slip on the deep megathrust, and significant slip rates are predicted both within and below the coseismic rupture zone. The WRMS velocity residual of the slip model is 1.5 mm/yr. The second model (Figure 3c) inverts for slip associated with residual velocities of the viscoelastic model that best-fit the observed horizontal GPS measurements (using the Paul *et al*. (2007) coseismic model and a 90 km elastic layer over a 3×10^{17} Pa s upper mantle viscosity). This produces more rapid slip of up to 1 m/yr, averaging ~ 50 cm/yr, and hence far exceeding likely rates of relative plate motion. The slip in this case is distributed fairly uniformly at depths immediately below the downdip terminus of coseismic rupture, which is where we would expect to find postseismic slip based on frictional properties. The WRMS of the combined viscoelastic and slip models is 4.0 mm/yr.

There is of course good reason to expect that viscoelastic rebound plays a significant role in the observed deformation. Large-scale uplift reflected in the GRACE geoid time-series and far-field deformation observed at GPS sites in Thailand and elsewhere cannot be explained by relatively small amounts of near-field moment release, so require a predominantly viscoelastic mechanism (Han *et al*., 2008; Pollitz *et al*., 2008; Panet *et al*., 2010; Einarsson *et al*., 2010), and any viscoelastic model consistent with these data would have a significant near-field deformation response. However, the results of our modeling here would suggest that near-field GPS measurements in the vicinity of the downdip terminus of great earthquake rupture might best be modeled as a combination of viscoelastic flow and deep postseismic slip downdip of the coseismic rupture, even many years after the event. Indeed, the 2004 Sumatra-Andaman event is not the only great subduction earthquake for which a significant component of long-term postseismic slip relaxation has been inferred from near-field geodetic data. Triangulation, tide gauge and leveling measurements collected after the March 27 1964, M_w = 9.2 Alaska event suggest both viscoelastic and postseismic slip are required to explain the transient deformation there (Brown *et al*., 1977; Suito and Freymueller, 2009).

One particularly intriguing piece of evidence relating to the deformation processes at work here is the consistency of the decay timescale of transient deformation: For example, both the near-field GPS deformation and the large-scale gravity exhibited early exponential decay with a timescale parameter of 0.7 to 0.8 years (e.g., Paul *et al*., 2007; de Linage *et al*., 2009). This would imply that the near-field and far-field deformation processes are either the same or closely coupled to one another. The latter would make physical sense in any case: Both postseismic slip models and viscoelastic relaxation models, in isolation, make naïve assumptions about the state and evolution of stress that neglect the likely significant influence of the other process on stress changes contributing to the response. For example stable frictional slip depends not on far-field parameters such as relative plate motion but rather on the very local time-derivative of stress (which, following an earthquake, is strongly conditioned by the viscoelastic deformation at greater depths). Similarly, viscoelastic flow will respond not only to the slip during an earthquake, but also to subsequent transient slip that is expected to occur downdip—and since it occurs much nearer the depths of viscoelastic flow than does the coseismic rupture, it will be particularly sensitive to the later slip if the moment release is a significant fraction of the coseismic, as suggested e.g. by Paul *et al*. (2007) and in recent modeling by Suito and Freymueller (2009), who suggest that up to 10% of the modern viscoelastic response to the great

1964 Alaska earthquake may relate to afterslip. Hence, closely-coupled postseismic deformation processes (and even similar decay timescales) are not just reasonable, they should be expected.

Conclusions

The most recent epochs of GPS data in the Andaman and Nicobar Islands, from four to six years after the M9.2 Sumatra-Andaman earthquake, still exhibit significant small-scale variations and large anomalous uplift rates that are significantly more consistent with a combination of viscoelastic flow and deep postseismic slip than with models consisting solely of viscoelastic flow in a radially-symmetric Earth. This may indicate either that postseismic slip still dominates the near-field signals, or that three-dimensional viscoelastic models proposed thus far inadequately capture the viscosity variations most salient to near-field deformation. Future modeling efforts should examine both viscoelastic flow and postseismic slip in combination, and particular attention should be paid to how stress changes resulting from each mechanism in isolation would be expected to perturb deformation behavior resulting from the other relaxation mechanism.

References

Altamimi, Z., X. Collilieux, J. Legrand, B. Garayt, and C. Boucher (2007). ITRF2005: A new release of the International Terrestrial Reference Frame based on time series of station positions and Earth Orientation Parameters, *J. Geophys. Res*. **112** #B09401, doi:10.1029/2007JB004949.

Banerjee, P., F.F. Pollitz, and R. Bürgmann (2005). The size and duration of the Sumatra-Andaman earthquake from far-field static offsets, *Science* **308** 1769–1772.

Banerjee, P., F. Pollitz, B. Nagarajan, and R. Bürgmann (2007). Coseismic slip distributions of the 26 December 2004 Sumatra-Andaman and 28 March 2005 Nias earthquakes from GPS static offsets, *Bull. Seism. Soc. Am*. **97** S86–S102.

Brown, L.D., R.E. Reilinger, S.R. Holdahl, and E.I. Balazs (1977). Postseismic crustal uplift near Anchorage, Alaska, *J. Geophys. Res*. **82** 3369–3378.

Cannelli, V., D. Melini, A. Piersanti, and E. Boschi (2008). Postseismic signature of the 2004 Sumatra earthquake on low-degree gravity harmonics, *J. Geophys. Res*. **113** #B12414.

Chen, J.L., C.R. Wilson, B.D. Tapley, and S. Grand (2007). GRACE detects coseismic and postseismic deformation from the Sumatra-Andaman earthquake, *Geophys. Res. Lett*. **34** #L13302.

Chlieh, M., J.P. Avouac, V. Hjorleifsdottir, T.R.A. Song, C. Ji, K. Sieh, A. Sladen, H. Hebert, L. Prawirodirdjo, Y. Bock, and J. Galetzka (2007). Coseismic slip and afterslip of the great M_w 9.15 Sumatra-Andaman earthquake of 2004, *Bull. Seism. Soc. Am.* **97** S152–S173.

Einarsson, I., A. Hoechner, R. Wang, and J. Kusche (2010). Gravity changes due to the Sumatra-Andaman and Nias earthquakes as detected by the GRACE satellites: a reexamination, *Geophys. J. Int*. **183** 733–747.

Gahalaut, V.K., B. Nagarajan, J.K. Catherine, and S. Kumar (2006). Constraints on 2004 Sumatra-Andaman earthquake rupture from GPS measurements in Andaman-Nicobar Islands, *Earth Planet. Sci. Lett*. **242** 365–374.

Gahalaut, V.K., J.K. Catherine, S. Jade, R. Gireesh, D.C. Gupta, M. Narsaiah, A. Ambikapathy, A. Bansal, and R.K. Chadha (2008). No evidence of unusually large postseismic deformation in Andaman region immediately after 2004 Sumatra-Andaman earthquake, *Geophys. Res. Lett*. **35** #L10307.

Gahalaut, V.K., S. Jade, J.K. Catherine, R. Gireesh, M.B. Ananda, P. Kumar, M. Narsaiah, S.S.H. Jafri, A. Ambikapathy, A. Bansal, R.K. Chadha, D.C. Gupta, B. Nagarajan, and S. Kumar (2008). GPS measurements of postseismic deformation in the Andaman–Nicobar region following the giant 2004 Sumatra–Andaman earthquake, *J. Geophys. Res.* **113** #B08401 doi:10.1029/2007JB005511.

Hashimoto, M., N. Choosakul, M. Hashizume, S. Takemoto, H. Takiguchi, Y. Fukuda, and K. Frjimori (2006). Crustal deformations associated with the great Sumatra-Andaman earthquake deduced from continuous GPS observation, *Earth Planets Space* **58** 127–139.

Herring, T. A. (2003), GLOBK: Global Kalman filter VLBI and GPS analysis program version 4.1, Mass. Inst. of Technol., Cambridge.

Jonsson, S., P. Segall, R. Pedersen, and G. Bjornsson (2003), Post-earthquake ground movements correlated to pore-pressure transients, *Nature* **424** 179–183.

Kayanne, H., Y. Ikeda, T. Echigo, M. Shishikura, T. Kamataki, K. Satake, J.N. Malik, S.R. Basir, G.K. Chakrabortty, and A.K.G. Roy (2007). Coseismic and postseismic creep in the Andaman Islands associated with the 2004 Sumatra-Andaman earthquake, *Geophys. Res. Lett*. **34** #L01310.

Kreemer, C., G. Blewitt, W.C. Hammond, and H.P. Plag (2006). Global deformation from the great 2004 Sumatra-Andaman Earthquake observed by GPS: Implications for rupture process and global reference frame, *Earth Planets Space* **58** 141–148.

Lay, T., H. Kanamori, C.J. Ammon, M. Nettles, S.N. Ward, R.C. Aster, S.L. Bilek, M.R. Brudzinski, R. Butler, H.R. Deshon, G. Ekstrom, K. Sataki, and S. Sipkin (2005) The great Sumatra-Andaman earthquake of 26 December 2004, *Science* **308** 1127–1133.

Liu, Y., and J. R. Rice (2007), Spontaneous and triggered aseismic deformation transients in a subduction fault model, *J. Geophys. Res.* **112** #B09404, doi: 10.1029/2007JB004930.

Meltzner, A.J., K. Sieh, M. Abrams, D.C. Agnew, K.W. Hudnut, J.P. Avouac, and D.H. Natawidjaja, Uplift and subsidence associated with the great Aceh-Andaman earthquake of 2004, *J. Geophys. Res., 111*(B02407), doi: 10.1029/2005JB003891, 2006.

Paul, J., A.R. Lowry, R. Bilham, S. Sen, and R. Smalley (2007). Postseismic deformation of the Andaman Islands following the 26 December, 2004, great Sumatra-Andaman earthquake, *Geophys. Res. Lett.* **34** #L19309, doi:10.1029/2007GL031024.

Paulson, A., S.J. Zhong, and J. Wahr (2005). Modeling post-glacial rebound with lateral viscosity variations, *Geophys. J. Int*. **163** 357-371.

Peltzer, G., P. Rosen, F. Rogez, and K. Hudnut (1998). Poroelastic rebound along the Landers 1992 earthquake surface rupture, *J. Geophys. Res*. **10** 30,131–30,145.

Pollitz, F.F., Gravitational-viscoelastic relaxation on a layered spherical Earth, *J. Geophys. Res.* **102** 17,921–17,941, 1997.

Pollitz, F.F., R. Bürgmann, and P. Banerjee (2006). Post-seismic relaxation following the great 2004 Sumatra-Andaman earthquake on a compressible self-gravitating Earth, *Geophys. J. Int.* **167** 397–420.

Pollitz, F., P. Banerjee, K. Grijalva, B. Nagarajan, and R. Bürgmann (2008). Effect of 3-D viscoelastic structure on post-seismic relaxation from the 2004 M = 9.2 Sumatra earthquake, *Geophys. J. Int.* **173** 189–204.

Rajendran, C.P., K. Rajendran, A. Earnest, R. Anu, T. Machado, and J. Freymueller (2007). The style of crustal deformation and seismic history associated with the 2004 Indian Ocean earthquake: A perspective from the Andaman-Nicobar Islands, *Bull. Seism. Soc. Am.* **97** doi: 10.1785/0120050630.

Rundle, J.B. (1978). Viscoelastic crustal deformation by finite, quasi-static sources, *J. Geophys. Res*. **83** 5937–5945.

Shearer, P., and R. Bürgmann (2010). Lessons learned from the 2004 Sumatra-Andaman megathrust rupture, *Annu. Rev. Earth Planet. Sci*. **38** 103–131.

Socquet, A., C. Vigny, N. Chamot-Rooke, W. Simons, C. Rangin, and B. Ambrosius (2006). India and Sunda plates motion and deformation along their boundary in Myanmar determined by GPS, *J. Geophys. Res*. **111** doi:10.1029/2005JB003877.

Suito, H., and J.T. Freymueller (2009). A viscoelastic and afterslip postseismic deformation model for the 1964 Alaska earthquake, *J. Geophys. Res*. **114** #B11404, doi:10.1029/2008JB005954.

Szeliga, W., T. I. Melbourne, M. M. Miller, and V. M. Santillan, Southern Cascadia episodic slow earthquakes, *Geophys. Res. Lett., 31,* L16602, doi: 10.1029/2004GL020824, 2004.

Tse, S.T., and J.R. Rice (1986). Crustal earthquake instability in relation to depth variation of frictional slip parameters, *J. Geophys. Res.* **91** 9452–9572.

Vigny, C., W.J.F. Simons, S. Abu, R. Bamphenyu, C. Satirapod, N. Choosakul, C. Subarya, A. Socquet, K. Omar, H.Z. Abidin, and B.A.C. Ambrosius (2005). Insight into the 2004 Sumatra-Andaman earthquake from GPS measurements in southeast Asia, *Nature* **436** 201–206.

Wessel, P., and W.H.F. Smith (1998). New, improved version of Generic Mapping Tools released, *Eos Trans. Am. Geophys. Un*. **79** 579.

Data and Resources

The GPS data presented here were collected by the lead author and the second author, and analyzed in the ITRF2005 reference frame using data from forty regional fiducial sites in the IGS archive. All raw GPS data from the NSF-funded Andaman and Nicobar postseismic network are archived for community download and use at the UNAVCO facility (http://www.unavco.org, 8/30/2011). Time series shown in Figure 2, and the other position time series used in this analysis, are available as an electronic supplement to this paper from the lead author's website at http://www.ceri.memphis.edu/people/jpuchkyl/anda2010.pdf (8/30/2011). All plots were made using the Generic Mapping Tools version 4.1.4 (http://www.soest.hawaii.edu/gmt; Wessel and Smith, 1998).

Acknowledgements

We thank Jeff Freymueller, Roland Bürgmann and an anonymous reviewer for constructive comments that greatly improved this manuscript. JP and ARL's efforts are funded by NSF grants EAR-0810084, EAR-0809954, EAR-1114268, and EAR-1114304. CPR is supported by the Ramanujan Fellowship, sponsored by the Department of Science and Technology, Government of India.